

Al-La-Ni Amorphous Alloys with a Wide Supercooled Liquid Region

By Akihisa Inoue*, Tao Zhang** and Tsuyoshi Masumoto*

Amorphous alloys exhibiting a wide supercooled liquid region and a high reduced glass transition temperature (T_g/T_m) were found to be formed over a compositional range from 3 to 83 at% La and 0 to 60%Ni in Al-La-Ni system by melt spinning. The temperature span $\Delta T_x (= T_x - T_g)$ between T_g and crystallization temperature (T_x) reaches as large as 69 K for $Al_{25}La_{55}Ni_{20}$. The T_g/T_m is also as high as 0.68 for $Al_{25}La_{55}Ni_{20}$ and the Al-La-Ni alloys are concluded to have a high glass-forming ability. The T_x and hardness (H_v) increase with increasing Al and Ni contents in the range from 425 K to 750 K and 170 to 520 and the tensile strength also has a similar compositional dependence in the range of 515 to 795 MPa. The compositional effect on T_x and H_v was presumed to originate from the variation of the atomic configuration which reflects the compounds of $La_3(Al, Ni)$, $La(Al, Ni)$ and $La(Al, Ni)_2$. The high stability of the supercooled liquid in the vicinity of the stoichiometric composition $Al_1La_2Ni_1$ against the transformation of crystalline phases, i.e., large ΔT_x and high T_g/T_m , seems to result from an optimum bonding state of the constituent atoms for the stoichiometric alloy.

(Received August 2, 1989)

Keywords: aluminum-lanthanum-nickel system, amorphous phase, liquid quenching, supercooled liquid, glass transition, mechanical strength, thermal stability

I. Introduction

From the viewpoint of the future progress of amorphous alloy bulks which can be produced by warm consolidation of amorphous powder or ribbon, it is important for an amorphous alloy to have simultaneously high strength, good ductility and wide temperature span $\Delta T_x (= T_x - T_g)$ between glass transition temperature (T_g) and crystallization temperature (T_x) reaching about 50 K. However, the amorphous alloy in which the third factor is satisfied is limited to two alloy systems of Pd-Ni-P and Pt-Ni-P in a great number of amorphous alloys reported up to date⁽¹⁾. The high thermal instability for most of amorphous alloys except the noble metal-based alloys has prevented the development of amorphous alloys to high-strength bulk materials probably because of the difficulty of warm consolidation resulting from small ΔT_x . It has recently been found⁽²⁾ that an amorphous $Mg_{50}La_{30}Ni_{20}$ alloy

prepared by liquid quenching exhibits the ΔT_x value of as large as 58 K, though the amorphous alloy fractures during bending deformation. This finding suggests the possibility of obtaining an amorphous alloy with large ΔT_x and good mechanical properties in some ternary alloy systems containing La and Ni elements. In searching for an amorphous alloy which is appropriate for the production of an amorphous bulk by consolidation in a supercooled liquid region between T_g and T_x , the present authors have found that the above-described three factors are satisfied in some Al-La-Ni amorphous alloys and the ΔT_x value of the alloys is as large as about 70 K. This paper is intended to clarify the composition range in which an amorphous phase is formed in rapidly solidified Al-La-Ni alloys and the thermal stability including the transition from the amorphous to crystalline phases through a supercooled liquid and the mechanical properties of the amorphous alloys.

II. Experimental Procedure

Binary Al-La and La-Ni and ternary Al-La-Ni alloys were used in the present study.

* Institute for Materials Research, Tohoku University, Sendai 980, Japan.

** Graduate Student, Tohoku University.

Their ingots were prepared by induction-melting a mixture of pure Al(99.99 mass%), La(99.9 mass%) and Ni(99.9 mass%) metals in a purified argon atmosphere. The compositions are nominally expressed in atomic per cent. From the master alloy ingots, ribbons with a cross section of about $0.02 \text{ mm} \times 1 \text{ mm}$ were prepared by a single roller melt-spinning technique in an argon atmosphere. The amorphicity of the melt-spun ribbons was examined by X-ray diffractometry and transmission electron microscopy techniques. The specific heat (C_p) associated with structural relaxation, glass transition and crystallization was measured with a differential scanning calorimeter (DSC). The accuracy of the data was about $\pm 0.4 \text{ J/mol-K}$ for absolute C_p values and better than $\pm 0.1 \text{ J/mol-K}$ for the relative C_p or ΔC_p measurements. The samples were first scanned at 0.67 K/s (40 K/min) to the temperature of the supercooled liquid to obtain data in the as-quenched state, and then cooled to room temperature. The $C_p(T)$ measurement was immediately repeated *in situ* to obtain the data on the control sample. This test procedure is essential in order to eliminate any possible error that might result from the drift in the calorimeter between the measurements. Hardness and tensile strength of the ribbon specimens were measured by a Vickers microhardness tester with a 0.98 N (100 gf) load and an Instron-type tensile testing machine at a strain rate of $4.17 \times 10^{-4} \text{ s}^{-1}$, respectively. Eight to ten symmetrical indentations and five tensile test data were used to determine the average microhardness value and tensile fracture strength. Tensile specimens were cut from the melt-spun ribbon into strips having a gauge dimension of 20 mm long for fracture strength. Subsequent to tensile testing, the cross-sectional area at the fracture site of each specimen was measured by optical microscopy and/or scanning electron microscopy in order to minimize error in the estimation of the tensile strength.

III. Results

Figure 1 shows the composition range in which an amorphous Al-La-Ni phase is formed by melt spinning, along with the data

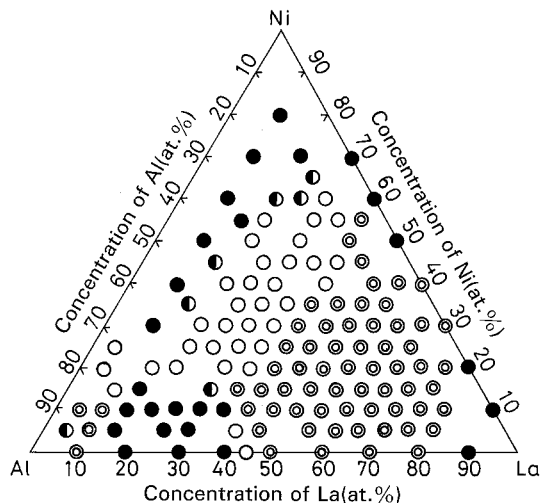


Fig. 1 Composition range for formation of amorphous phase in Al-La-Ni system: (⊙) amorphous (ductile); (○) amorphous (brittle); (●) amorphous and crystalline; (●) crystalline.

of bending ductility of the amorphous alloys. The glass formation range is quite wide and can be divided into two categories of Al-rich and La-rich compositions; 3 to 18 at% La and 0 to 15%Ni for the Al-rich alloys and 20 to 83%La and 0 to 60%Ni for the La-rich alloys. In addition, it is seen in Fig. 1 that binary amorphous alloys are formed in the Al-La and La-Ni systems. It is thus to be noted that the Al-La-Ni alloys can be amorphized over a wide compositional range which is comparable to about 60 to 70% in area in the entire compositional range of the ternary system. Figure 1 also shows that ductile amorphous alloys, which can be bent through 180 degrees without fracture, are obtained in the Al-rich range of 3 to 13%La and 0 to 12%Ni and in the La-rich range of 35 to 83%La and 0 to 55%Ni. One can see a tendency that an approach of alloy composition to $(\text{Al, Ni})_2\text{La}$ brings about the transition from the ductile to brittle nature of the Al-La-Ni amorphous alloys. Figure 2 shows the compositional dependence of crystallization temperature (T_x) for the Al-La-Ni amorphous alloys. The T_x value is in the range of 425 to 500 K for the La-rich alloys containing above about 60%La, increases significantly with increasing Al and Ni contents and reaches 750 K for $\text{Al}_{50}\text{La}_{20}\text{Ni}_{30}$. With a further increase

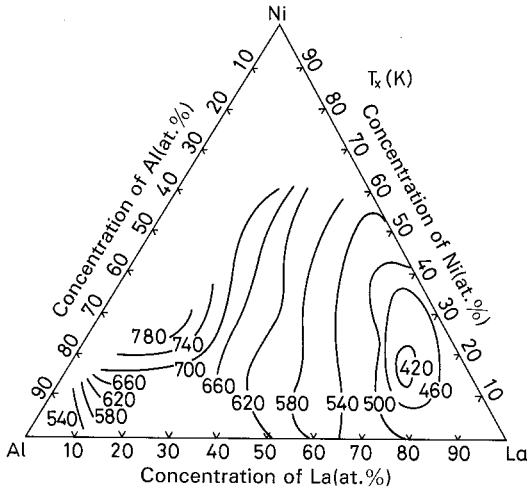


Fig. 2 Compositional dependence of crystallization temperature (T_x) of Al-La-Ni amorphous alloys.

in Al content, T_x decreases significantly to 542 K for $\text{Al}_{85}\text{La}_5\text{Ni}_{10}$. As is evident from the contour lines of T_x in Fig. 2, the T_x values of the Al-La-Ni amorphous alloys except the Al-rich alloys are mainly dominated by the Al and Ni contents and there is no distinct difference between the compositional effects of Al and Ni elements on T_x .

As examples, Fig. 3 shows the DSC curves of $\text{Al}_{45-x}\text{La}_{55}\text{Ni}_x$ ($x=15, 20$ and 25 at%) amorphous alloys. It is seen that the three alloys crystallize through a single stage accompanied by an exothermic heat ranging from 4.82 to 5.14 kJ/mol. In addition to the exothermic peak, one can notice an endothermic reaction with a very wide temperature span in the temperature range below the onset temperature (T_x) of crystallization. For instance, the $\text{Al}_{25}\text{La}_{55}\text{Ni}_{20}$ amorphous alloy begins to transform from the amorphous solid to a supercooled liquid at about 465 K and keeps the supercooled liquid state in a wide temperature span reaching about 70 K, followed by crystallization at 545 K. As the largest temperature span of the supercooled liquid region for amorphous metallic materials is known to be about 60 K for Pt-Ni-P⁽³⁾, 50 K for Pd-Ni-P⁽³⁾ and 58 K for Mg-Ni-La⁽²⁾, it is believed that the $\text{Al}_{25}\text{Ni}_{25}\text{La}_{50}$ alloy has the largest ΔT_x value in all amorphous alloys.

Figure 4 shows the compositional effect on

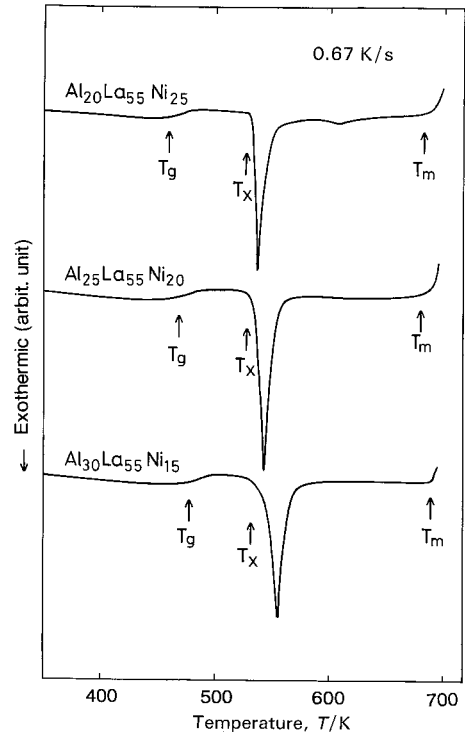


Fig. 3 Differential scanning calorimetric (DSC) curves of $\text{Al}_{45-x}\text{La}_{55}\text{Ni}_x$ ($x=15, 20$ and 25 at%) amorphous alloys.

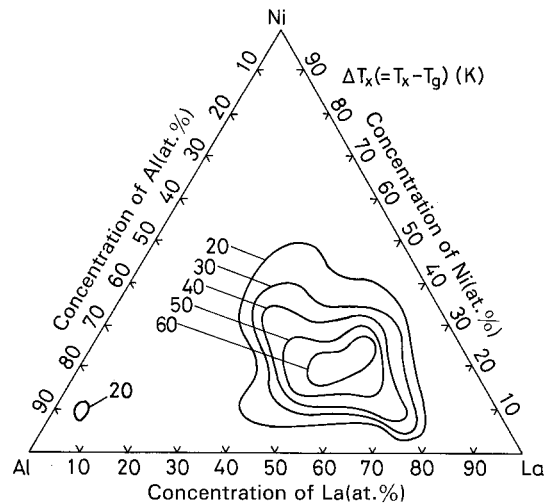


Fig. 4 Compositional dependence of the temperature span ΔT_x between T_g and T_x of Al-La-Ni amorphous alloys.

the ΔT_x value for the Al-La-Ni amorphous alloys. The ΔT_x value is maximum (69 K) for $\text{Al}_{25}\text{La}_{55}\text{Ni}_{20}$ and decreases with a deviation

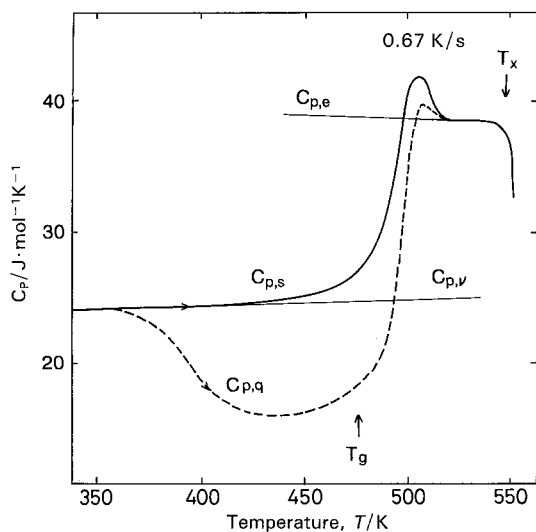


Fig. 5 The thermogram $C_{p,q}(T)$ of an amorphous $\text{Al}_{25}\text{La}_{55}\text{Ni}_{20}$ alloy in the as-quenched state. The solid line represents the thermogram $C_{p,s}(T)$ of the sample heated to 520 K.

from the alloy component. However, it is notable that the T_x value above 50 K is obtained in the range from 40 to 65%La and 13 to 30%Ni and the glass transition phenomenon is observed over a wide compositional range from 25 to 78%La and 5 to 50%Ni.

In order to examine the change of the specific heat by the transition of an amorphous solid to a supercooled liquid and the temperature dependence of the specific heat in the amorphous solid and supercooled liquid, the detailed differential scanning calorimetric measurement was made for the Al–La–Ni amorphous alloys. As an example, Fig. 5 shows the thermograms of an amorphous $\text{Al}_{25}\text{La}_{55}\text{Ni}_{20}$ alloy with the widest supercooled liquid region. The C_p value of the as-quenched phase is 24 J/mol·K near room temperature. As the temperature rises, the C_p value increases gradually and begins to decrease, indicating an irreversible structural relaxation at about 355 K. With a further increase in temperature, the C_p value reaches its minimum at about 430 K, then increases rapidly in the glass transition range from 465 to 495 K and reaches 38.4 J/mol·K for the supercooled liquid around 515 K. With further increased temperature, the C_p value of the supercooled liquid decreases

gradually and then rapidly due to crystallization at 545 K. It is seen in Fig. 5 that the transition of the amorphous solid to the supercooled liquid takes place accompanied by a large increase in the specific heat, $\Delta C_{p,s \rightarrow l}$, reaching 14 J/mol·K. The difference in $C_p(T)$ between the as-quenched and the reheated states, $[\Delta C_p(T)]$, manifests the irreversible structural relaxation which is presumed to arise from the annihilation of various kinds of quenched-in “defects” and the enhancement of the topological and chemical short-range ordering through the atomic rearrangement. The details of the structural relaxation behavior will be described elsewhere.

The $C_{p,s}$ curve of the reheated (control) sample is unaffected by thermal changes and consists of configurational contributions as well as those arising from purely thermal vibrations. Therefore, the vibrational specific heat, $C_{p,v}$, for the amorphous alloy is extrapolated from the C_p values in the low temperature region and is a linear function of temperature, viz.,

$$C_{p,v} = 24.2 + 4.65 \times 10^{-4}(T - 360) \quad 360 \leq T \leq 425. \quad (1)$$

Similarly, the equilibrium specific heat, $C_{p,e}$, of the supercooled liquid, including the vibrational and configurational specific heat, can be expressed by eq. (2) based on the data shown in Fig. 5,

$$C_{p,e} = 38.4 + 5.11 \times 10^{-4}(540 - T) \quad 517 \leq T \leq 545. \quad (2)$$

The $\Delta C_{p,s \rightarrow l}$ value for the Al–La–Ni amorphous alloys was examined as a function of composition. As a result, it was found that the $\Delta C_{p,s \rightarrow l}$ value is about 14 J/mol in the vicinity of $\text{Al}_{25}\text{La}_{55}\text{Ni}_{20}$ and tends to decrease with a deviation from the alloy composition, being similar to the compositional dependence of ΔT_x . That is, there is a tendency that the larger the ΔT_x the larger is the $\Delta C_{p,s \rightarrow l}$. The $\Delta C_{p,s \rightarrow l}$ values are nearly equal to those for Pt–Ni–P⁽³⁾, Pd–Ni–P⁽³⁾ and Mg–Ni–La⁽²⁾ amorphous alloys.

It is important to examine the reduced glass transition temperature (T_g/T_m) for the Al–La–Ni amorphous alloys exhibiting the wide super-

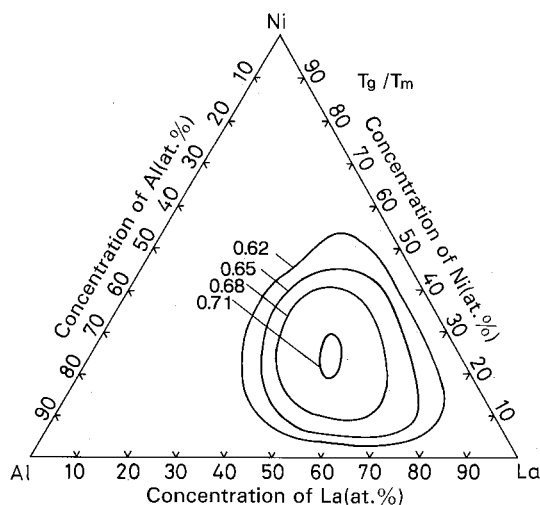


Fig. 6 Compositional dependence of the reduced glass transition temperature (T_g/T_m) of Al-La-Ni amorphous alloys.

cooled liquid region. As shown in Fig. 3, the onset temperature of fusion can be accurately measured from the DSC curve. When the onset temperature of the endothermic reaction in the temperature range above T_x is regarded as a melting temperature (T_m), the T_g/T_m value can be evaluated. Figure 6 shows the compositional effect on the T_g/T_m value for the Al-La-Ni amorphous alloys. The T_g/T_m value is about 0.71 in the vicinity of 50%La and 25%Ni and decreases gradually with a deviation from the composition. Thus, there is a clear tendency that the higher the T_g/T_m value, the larger are the ΔT_x and $\Delta C_{p,s \rightarrow l}$.

Vickers hardness (H_v) and tensile fracture strength (σ_f) were measured for the ductile Al-La-Ni amorphous alloys exhibiting large values of ΔT_x , $\Delta C_{p,s \rightarrow l}$ and T_g/T_m . Figure 7

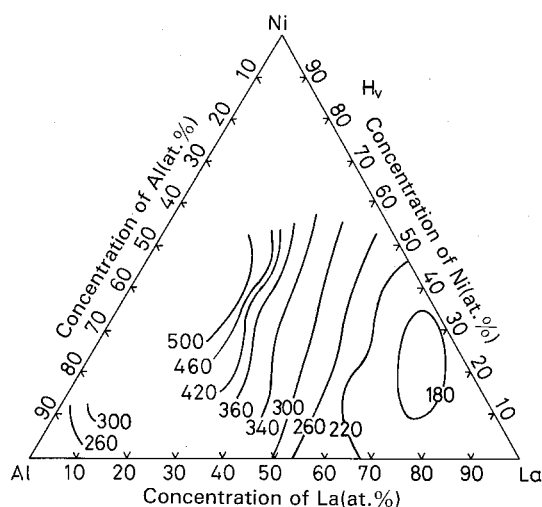


Fig. 7 Compositional dependence of Vickers hardness number (H_v) of Al-La-Ni amorphous alloys.

shows the compositional effect on the H_v for the Al-La-Ni amorphous alloys. The H_v number is about 180 in the vicinity of 70%La and 15%Ni, increases significantly with increasing Al and Ni contents and reaches a maximum value of 520 in the vicinity of 40%Al and 40%Ni. Thus, the increase of the H_v value with an increase of Al and Ni contents is more remarkable in the condition of Al/Ni \approx 1.0. The feature of the compositional effect on H_v is very analogous to those for T_g and T_x .

A similar compositional effect was also recognized for the tensile fracture strength (σ_f) and Young's modulus (E). As summarized in Table 1, the σ_f and E values increase with increasing Al and Ni contents from 515 to 795 MPa and 33.8 to 52.3 GPa, respectively. Here, it should be pointed out that the properties of $\sigma_f > 700$ MPa, $E > 50$ GPa, $\Delta C_{p,s \rightarrow l} > 10$ J/mol-

Table 1 Mechanical properties of Al-La-Ni amorphous alloys.

Alloy (at%)	σ_f (MPa)	E (GPa)	H_v	$\epsilon_{t,f} = \sigma_f/E$	$\epsilon_{c,y} \approx 9.8H_v/3E$	$\sigma_{c,y} \approx 9.8H_v/3$ (MPa)
Al ₄₅ La ₄₅ Ni ₁₀	795	52.3	330	0.015	0.021	1080
Al ₃₅ La ₄₅ Ni ₂₀	720	46.3	305	0.016	0.022	995
Al ₃₅ La ₅₀ Ni ₁₅	715	41.1	290	0.017	0.023	950
Al ₃₀ La ₅₀ Ni ₂₀	715	41.3	285	0.017	0.023	930
Al ₂₅ La ₅₅ Ni ₂₀	515	33.8	225	0.015	0.022	735

Tensile fracture strength (σ_f), Young's modulus (E), Vickers hardness (H_v), tensile fracture strain ($\epsilon_{t,f} = \sigma_f/E$), compressive yield strain ($\epsilon_{c,y} \approx 9.8H_v/3E$) and compressive yield strength ($\sigma_{c,y} \approx 9.8H_v/3$).

K and $T_g/T_m > 0.68$ are satisfied simultaneously for some amorphous alloys in the Al-La-Ni system.

IV. Discussion

1. Compositional effect on T_x , H_v , E and σ_f

It was shown in section III that the T_x , H_v , E and σ_f values of the Al-La-Ni amorphous alloys have the same compositional effect and increase with increasing Al and Ni contents. The maximum values of T_x , H_v and E are obtained in the vicinity of $(\text{Al, Ni})_2\text{La}$, accompanied by the ductile to brittle transition, and the increase in T_x , H_v and E is the largest when the concentration ratio of Al to Ni is nearly 1.0. Although the atomic configuration of the Al-La-Ni amorphous alloys remains unclear, it is interpreted that the simultaneous existence of the solute elements (Al and Ni) in the La base amorphous alloys brings about the increase in T_x , H_v and E . Although there is no equilibrium phase diagram available in the Al-La-Ni ternary alloys, the binary phase diagrams of La-Al⁽⁴⁾ and La-Ni⁽⁵⁾ alloys indicate that the increase in T_x , H_v and E corresponds well to the significant increase in T_m from 823 to 1678 K for the La-Al system and from 758 to 1598 K for the La-Ni system, accompanied by the structural changes of $\text{La}_3\text{Al} \rightarrow \text{LaAl} \rightarrow \text{LaAl}_2$ and $\text{La}_3\text{Ni} \rightarrow \text{LaNi} \rightarrow \text{LaNi}_2$. From the similarities of the chemical formula and crystal structure of their compounds in the La-Al and La-Ni systems, it is reasonable to consider that the compounds in the Al-La-Ni ternary system change in the order of $\text{La}_3(\text{Al, Ni}) \rightarrow \text{La}(\text{Al, Ni}) \rightarrow \text{La}(\text{Al, Ni})_2$ with increasing Al and Ni contents, accompanied by the significant increase in T_m . Although the amorphous structure of the Al-La-Ni alloys remains unclear, it is presumed that the atomic configuration on a short-range scale varies with the sequence change in the equilibrium compounds. That is, the amorphous structure reflects the $\text{La}_3(\text{Al, Ni})$ with the lowest T_m in the La-rich compositional range and the increase in the Al and Ni contents gives the variation into the amorphous structure which reflects the $\text{La}(\text{Al, Ni})$ and

$\text{La}(\text{Al, Ni})_2$ compounds with higher T_m . Accordingly, the monotonous and significant increases in T_x , H_v , E and σ_f with Al and Ni contents may be explained by the variation of the short-range atomic configuration which reflects the change of the equilibrium compounds of $\text{La}_3(\text{Al, Ni}) \rightarrow \text{La}(\text{Al, Ni}) \rightarrow \text{La}(\text{Al, Ni})_2$. The entire replacement between Al and Ni for the La_3M , LaM and LaM_2 seems to be possible because of the similar types of the chemical formula and crystal structure of the three compounds between the La-Al⁽⁴⁾ and La-Ni⁽⁵⁾ systems. It is expected from a common concept for the solid solution that the achievement of the entire replacement gives the maximum values of T_x and H_v in the compositional range where the concentration ratio of Al to Ni is nearly 1.0. Furthermore, the attractive bonding nature between Al and Ni atoms is thought to play an important role in the increase in T_x , H_v , E and σ_f with increasing Al and Ni contents. The attractive bonding nature is also expected to be the largest in the vicinity of $\text{Al/Ni} \approx 1.0$, because of the highest T_m value at 50%Ni⁽⁶⁾ in Al-Ni binary system. The compositional effect of the attractive bonding nature between Al and Ni is presumed to bring about the compositional dependence in which the T_x and H_v show their maximum values at $\text{Al/Ni} \approx 1.0$.

A similar concept can be applied to explain the compositional dependences of T_x and H_v in the Al-rich amorphous alloys. The Al-rich binary phase is formed in the vicinity of $\text{Al}_{90}\text{La}_{10}$ ⁽⁷⁾ and the Al-Ni binary alloys cannot be amorphized⁽⁸⁾. It is therefore thought that the glass formation in the Al-rich Al-La-Ni alloys is mainly dominated by the attractive bonding nature between Al and La atoms. The T_m of Al-La binary alloys decreases significantly from 1678 to 913 K with decreasing La content from 33.3 to 2.5%⁽⁴⁾. The compositional effect on T_x and H_v for the Al-rich amorphous alloys is similar to that for T_m and hence the decrease of T_x and H_v for the Al-La-Ni amorphous alloys with a further increase in La content from about 30 to 80 at% seems to result from the short-range atomic configuration which reflects the change of the equilibrium phases leading to the decrease in T_m . Clarifica-

tion of the short-range atomic configuration to confirm the above-described concept is in progress for the Al-La-Ni amorphous alloys.

2. Compositional effect on ΔT_x and T_g/T_m

The supercooled liquid region at temperatures below T_x was observed in wide compositional ranges of 25 to 78%La and 5 to 50%Ni for the La-rich alloys and 5 to 9%La and 8 to 12%Ni for the Al-rich alloys. It is particularly notable that the temperature span (ΔT_x) of the supercooled liquid is as large as 69 K in the vicinity of 50%La and 20%Ni. Furthermore, it is shown in Fig. 6 that the amorphous alloys with the large ΔT_x values have high T_g/T_m values reaching about 0.7. The large values of ΔT_x and T_g/T_m indicate that the supercooled liquid of the Al-La-Ni amorphous alloys has a high stability to the nucleation and growth of the crystalline phases. The retardation of the transformation to a crystalline phase for the supercooled liquid is thought to bring about the high values of ΔT_x and T_g/T_m . The reason why the large values of ΔT_x and T_g/T_m are obtained in the vicinity of $\text{Al}_{25}\text{La}_{50}\text{Ni}_{25}$ is discussed in this section. The equilibrium phase diagrams of La-Al⁽⁴⁾ and La-Ni⁽⁵⁾ binary alloys show the existence of a deep trough in the vicinity of 70%La, indicating a high stability of the liquidus structure at their alloy compositions. The ratios of Al to La and Ni to La at the compositions are nearly equal to those for the $\text{Al}_{25}\text{La}_{50}\text{Ni}_{25}$ alloy with the largest ΔT_x and T_g/T_m values. The agreement suggests that the liquidus structure is more stable in the vicinity of $\text{Al}_{25}\text{La}_{55}\text{Ni}_{20}$. The existence of the deep trough suggests an ease of obtaining a supercooled state probably because of the high stability of the supercooled liquid at the composition. Thus, the equilibrium phase diagrams allow us to presume that the high stability of the supercooled liquid is closely related to an ease of supercooling of the liquid state. Although a number of eutectic-type alloy systems have an easy supercooling capacity of liquid, no amorphous alloys with large ΔT_x have been obtained in most of the eutectic-type alloys⁽⁹⁾. The exceptionally high stability of the supercooled liquid in the Al-La-Ni system seems to be attributed to the unique bonding

state of the Al-La-Ni amorphous alloys. The electronic structure and bonding nature of the Al-La-Ni amorphous alloys are also under investigation.

3. Glass-forming capacity

As described above, the large ΔT_x values imply that the supercooled liquid can exist in a wide temperature range without crystallization and has a high resistance to the nucleation and growth of crystalline phases. The high resistance also implies that the supercooled liquid obtained by melt spinning can also have a high resistance to the nucleation and growth of crystalline phases, leading to a high glass-forming capacity, though the origin for the high resistance of the Al-La-Ni alloys remains unknown. It is known that the T_g/T_m value is closely related to the glass-forming capacity and the higher the T_g/T_m value the larger is the glass-forming capacity. The empirical relation⁽¹⁰⁾ between T_g/T_m and the maximum cooling rate for the formation of an amorphous phase allows us to evaluate that the minimum cooling rate for the $\text{Al}_{25}\text{La}_{55}\text{Ni}_{20}$ alloy is as small as about 10^2 K/s. The cooling rate is almost comparable to that which can be achieved even by water quenching, suggesting the possibility of obtaining an amorphous bulk by water quenching. The possibility has been confirmed by the evidence⁽¹¹⁾ that an amorphous $\text{Al}_{25}\text{La}_{50}\text{Ni}_{25}$ alloy with a cylindrical form in the diameter range below 1.2 mm is formed by water quenching.

The high T_g/T_m value also implies that the viscosity of the supercooled liquid can reach about 10^{14} N·s/m² by a lower degree of supercooling. It is thus said that the temperature dependence of viscosity of the supercooled liquid is very steep. The steep increase of viscosity with decreasing temperature is presumably due to a rapid increase in the difficulty of the diffusivity of the constituent atoms. The difficulty of the diffusivity is thought to take place by the achievement of a tight bonding state of the constituent atoms. Considering that the alloys exhibiting the largest values of ΔT_x and T_g/T_m are located in the vicinity of $\text{Al}_{25}\text{La}_{50}\text{Ni}_{25}$ (AlLa_2Ni), the short-range atomic configuration which reflects the stoichiometric

$\text{Al}_1\text{La}_2\text{Ni}_1$ compound may be favorable for the suppression of the diffusivity of the constituent atoms. Research of the atomic configuration of the $\text{Al}_1\text{La}_2\text{Ni}_1$ amorphous alloy with a stoichiometric composition is expected to shed some light on the clarification of the mechanism for the appearance of large values of ΔT_x and T_g/T_m .

V. Summary

In order to find amorphous alloys exhibiting high mechanical strengths, a wide supercooled liquid region and a high glass-forming capacity in Al-containing systems by liquid quenching, the rapidly solidified structure in the Al-La-Ni ternary system was examined over a wide compositional range. The amorphous alloys are formed in a wide compositional range which extends from the Al-rich to the La-rich composition of 3 to 83%La and 0 to 60%Ni. Furthermore, the Al-La-Ni amorphous alloys exhibit a supercooled liquid region in each range of 5 to 9%La and 8 to 12%Ni for the Al-rich alloys and 25 to 78%La and 5 to 50%Ni for the La-rich alloys. In particular, the alloys which are located in the vicinity of 55%La and 20%Ni have large temperature spans $\Delta T_x (= T_x - T_g)$ reaching about 70 K and high T_g/T_m values above 0.7. The ΔT_x and T_g/T_m values are believed to be the largest in metallic amorphous materials. The large values of ΔT_x and T_g/T_m indicate that the supercooled liquid has the high stability of the transformation to a crystalline phase and viscosity increases steeply with increasing degree of supercooling. The high stability of the supercooled liquid and the steep increase of viscosity are explained by the presumption that the amorphous structure is

in an optimally bonding state which reflects the stoichiometric compound $\text{Al}_1\text{La}_2\text{Ni}_1$. The T_x and H_v of the La-rich amorphous alloys increase from 425 to 750 K and 170 to 520 with increasing Al and Ni contents and the increase is more remarkable for the alloys containing an equivalent concentration of Al and Ni. The E and σ_f values also show a similar compositional effect and the highest σ_f value is about 795 MPa. The compositional effect on T_x , H_v , E and σ_f is presumed to result from the change in the short-range atomic configuration which reflects the change of the equilibrium $\text{La}_3(\text{Al}, \text{Ni})$, $\text{La}(\text{Al}, \text{Ni})$ and $\text{La}(\text{Al}, \text{Ni})_2$ compounds because the T_m increases from 823 to 1678 K in the order of La_3Al , LaAl and LaAl_2 and from 788 to 1100 K in the order of La_3Ni , LaNi and LaNi_2 .

REFERENCES

- (1) H. S. Chen: Rep. Prog. Phys., **43** (1980), 353.
- (2) A. Inoue, M. Kohinata, K. Ohtera, A. P. Tsai and T. Masumoto: Mater. Trans., JIM, **30** (1989), 378.
- (3) H. S. Chen, Mater. Sci. Eng., **23** (1976), 151.
- (4) K. A. Gschneidner, Jr. and F. W. Calderwood: *Binary Alloy Phase Diagrams*, ed. T.B. Massalski, ASM, Ohio, (1986), p. 125.
- (5) M. Hansen: *Constitution of Binary Alloys*, McGraw-Hill, New York, (1958), p. 857.
- (6) M. F. Singleton, J. L. Murray and P. Nash: *Binary Alloy Phase Diagrams*, ed. T.B. Massalski, ASM, Ohio, (1986), p. 125.
- (7) A. Inoue, K. Ohtera and T. Masumoto: Jpn. J. Appl. Phys., **27** (1988), L736.
- (8) A. Inoue, K. Ohtera, A. P. Tsai and T. Masumoto: Jpn. J. Appl. Phys., **27** (1988), L280.
- (9) *Materials Science of Amorphous Metals*, ed. T. Masumoto *et al.*, Ohm Pub., Tokyo, (1982), p. 28.
- (10) H. A. Davies: *Amorphous Metallic Alloys*, ed. F. E. Luborsky, Butterworths, London, (1983), p. 8.
- (11) A. Inoue, K. Kita, T. Zhang and T. Masumoto: Mater. Trans., JIM, **30** (1989), 722.